

Does Λ CDM really be in tension with the Hubble diagram data?

Ahmad Mehrabi¹ and Spyros Basilakos²

¹*Department of Physics, Bu-Ali Sina University, Hamedan 65178, 016016, Iran**

²*Academy of Athens, Research Center for Astronomy & Applied Mathematics, Soranou Efessiou 4, 11-527, Athens, Greece[†]*

(Dated: July 21, 2020)

In this article, we elaborate further on the Λ CDM "tension", suggested recently by the authors [1, 2]. We combine Supernovae type Ia (SNIa) with quasars (QSO) and Gamma Ray Bursts (GRB) data in order to reconstruct in a model independent way the Hubble relation to as high redshifts as possible. Specifically, in the case of either SNIa or SNIa/QSO data we find that current values of the cosmokinetic parameters extracted from the Gaussian process are consistent with those of Λ CDM. Including GRBs in the analysis we find a tension, which however is not as significant as that mentioned in [1, 2]. Finally, we argue that the choice of the kernel function used in extracting the luminosity distance might affect the amount of tension.

I. INTRODUCTION

Since the discovery of the accelerated expansion of the Universe from the Supernovae type Ia (SNIa) data [3, 4], the combined analysis of various cosmological probes, including those of Cosmic Microwave Background (CMB) [5–7], Baryon Acoustic Oscillation (BAO) [8–14] and cosmic chronometers [15] confirms the aforementioned dynamical result, namely that currently the Universe accelerates. However, the physics of cosmic acceleration is still a mystery, hence the aim in these kind of studies is to provide an explanation regarding the underlying mechanism which triggers such a phenomenon.

In the framework of homogeneous and isotropic Universe, the accelerated expansion can be described by considering either an exotic matter with negative pressure [16–22] or a modification of gravity [$f(R)$ theories and the like, 23–27]. Among the large family of dark energy and modified gravity models, the simplest case is the spatially flat Λ CDM model for which cold dark matter (CDM) and baryonic matter coexist with the cosmological constant. From the theoretical viewpoint, the Λ CDM model suffers from the well known problems, namely the coincidence and the expected value of the vacuum energy density [28–31].

On the other hand, despite the fact that the Λ CDM model is found to be in a very good agreement with the majority of cosmological data [7], nonetheless the model seems to be currently in tension with some recent measurements [32–35], related with the Hubble constant H_0 and the present value of the mass variance at $8h^{-1}$ Mpc, namely σ_8 . Moreover, Lusso *et al.* [1] using a combined Hubble diagram of SNIa, Quasars, and gamma-ray bursts (GRBs) found a $\sim 4\sigma$ tension between the best fit cosmographic parameters with respect to those of Λ CDM (see also [2, 36]). In the light of the latter results, a heated debate is taking place in the literature and the aim of the present article is to contribute to this debate.

Here, we focus on a model-independent parametrization of the Hubble diagram using the Gaussian process, and investigate its performance against the latest Hubble diagram data. Notice that in this case we need to introduce a kernel function with some hyperparameters which can be optimized in order to fit the data. For more details concerning model-independent methods we refer to [37–40]. The structure of the paper is as follows. In section II, we introduce the concept of the Gaussian process and we present the corresponding kernel functions that we shall use in the current work. In section III, we discuss the observational data and the procedure of our analysis, while in section IV we provide our results. Finally, in V, we summarize our results and we draw our conclusions.

II. MODEL INDEPENDENT METHOD- GAUSSIAN PROCESS

We consider that the universe is a self-gravitating fluid, endowed with a spatially flat homogeneous and isotropic geometry. In this context, there are two main approaches in order to investigate cosmological data e.g. the luminosity distance. In the first case we impose a cosmological model, hence we estimate the form of the luminosity distance. Then we fit the model to data in order to place constraints on the corresponding parameter space. This is a model-dependent method in a sense that different models provide different forms of luminosity distance. Another avenue is to utilize a model independent method in reconstructing the Hubble diagram through the observational data [37–40]. In this approach we do not need to know apriori the

*Electronic address: mehrabi@ipm.ir

[†]Electronic address: svasil@academyofathens.gr

underlying cosmological model. One of the most popular model independent method is the Gaussian process (GP), hence in the present article we test the performance of GP against the available Hubble diagram data.

Briefly, the main steps of the method are the following. Having a data set D

$$D = \{(x_i, y_i) | i = 1, \dots, n\}, \quad (1)$$

our aim is to reconstruct in a model independent way a function $f(x)$ which describes the data. In this case at any point x , the value $f(x)$ is a Gaussian random variable with mean $\mu(x)$ and variance $Var(x)$. Moreover, the function values at any two different points are not independent from each other, hence the covariance function $cov(f(x), f(\tilde{x})) = k(x, \tilde{x})$ describes the corresponding correlations. Therefore, having an observational data set (x_i, y_i) and considering a kernel function $k(x, \tilde{x})$, it is straightforward to compute the value of function and its covariance (for more detail see [41]). Concerning the functional form of the kernel, there is a wide range of possibilities. In the current work we restrict our analysis to the following parametrizations:

$$k(x, \tilde{x}) = \sigma_f^2 \exp\left(-\frac{(x - \tilde{x})^2}{2l^2}\right), \quad (2)$$

$$k(x, \tilde{x}) = \sigma_f^2 \exp\left(-\sqrt{7}\frac{|x - \tilde{x}|}{l}\right)\left(1 + \sqrt{7}\frac{|x - \tilde{x}|}{l} + 14\frac{(x - \tilde{x})^2}{5l^2} + 7\sqrt{7}\frac{|x - \tilde{x}|^3}{15l^3}\right), \quad (3)$$

and

$$k(x, \tilde{x}) = \sigma_f^2 \exp\left(-3\frac{|x - \tilde{x}|}{l}\right)\left(1 + 3\frac{|x - \tilde{x}|}{l} + 27\frac{(x - \tilde{x})^2}{7l^2} + 18\frac{|x - \tilde{x}|^3}{7l^3} + 27\frac{(x - \tilde{x})^4}{35l^4}\right). \quad (4)$$

Notice that (3) and (4) are the so called Matern ($\nu = 7/2$ and $\nu = 9/2$) formulas respectively. It is worth noting that the family of Matern kernels is a generalization of kernel (2) and it is widely used in multivariate statistical analysis. In this case the absolute exponential kernel is parameterized by an additional parameter ν . If ν goes to infinity then the kernel reduces to Eq.(2), while in the case of $\nu = 1/2$ the kernel becomes equivalent to the absolute exponential kernel. Also σ_f and l are two hyperparameters which can be constrained from the observational data. Since the kernel function plays a role in reconstructing $f(x)$ (in our case comoving distance), we have decided to use the aforementioned kernels in order to test whether the choice of the kernel can affect the amount of the so called Λ CDM cosmokinetic tension.

Here we use the GAPP code [41] in order to reconstruct $f(x)$ and its derivatives. Specifically, $f(x)$ and its derivatives are given by

$$f(x) \sim GP(\mu(x), k(x, \tilde{x})) \quad (5)$$

$$f'(x) \sim GP(\mu'(x), \frac{\partial^2 k(x, \tilde{x})}{\partial x \partial \tilde{x}}) \quad (6)$$

$$f''(x) \sim GP(\mu''(x), \frac{\partial^4 k(x, \tilde{x})}{\partial^2 x \partial^2 \tilde{x}}), \quad (7)$$

where GP stands for Gaussian process.

III. OBSERVATIONAL DATA AND METHOD

The luminosity distance is the ideal tool to investigate the Hubble diagram. Our aim is to extend the Hubble relation to as high redshifts as possible, hence in addition to SNIa, we also consider QSOs and GRBs. In particular, bellow we briefly present the type of standard candles, used in the statistical analysis.

- *Supernovae (SNIa)*: we utilize the ‘‘Pantheon’’ compilation of SNIa data [42]. This sample contains 1048 spectroscopically confirmed SNIa in the redshift range $0.01 < z < 2.26$.
- *Quasars (QSOs)*: Furthermore, we use the sample of 1598 QSOs as collected by [2, 43]. The redshift interval of the current data is $0.04 < z < 5.1$. Notice that, in our analysis we use bin-averaged version of QSOs data.
- In addition to the above data, we use a compilation of 162 GRBs [44–46] in the range of $0.03 < z < 9.3$. Unlike SNIa, QSOs and GRBs are observed up to very high redshifts ($z > 3$) at which the distance modulus is more sensitive to the cosmological parameters [47].

The evolution of the distance modulus is given by $\mu(z) = 5\log D_L(z) + 25$, hence

$$D_L(z) = 10^{(\mu(z)-25)/5}, \quad (8)$$

where $D_L(z)$ is the luminosity distance from which the normalized comoving distance ¹ is written as

$$D(z) = \frac{H_0}{c} \frac{D_L(z)}{1+z}. \quad (9)$$

Notice that H_0 is the Hubble constant and c is the speed of light.

Based on the above, we compute the normalized comoving distance data points and then we use them in order to reconstruct the form of $D(z)$ as well as its derivatives. As a matter of fact knowing $D(z)$ and its derivatives, it is straightforward to compute the Hubble function $H(z)$ as well as its first and second derivatives, namely

$$H(z) = \frac{H_0}{D'(z)}, \quad (10)$$

$$H'(z) = -H_0 \frac{D''(z)}{D'(z)^2}, \quad (11)$$

$$H''(z) = H_0 \left[\frac{2D''(z)^2}{D'(z)^3} - \frac{D'''(z)}{D'(z)^2} \right]. \quad (12)$$

Moreover using the error propagation we obtain

$$\delta H(z) = H_0 \frac{\delta D'(z)}{D'(z)^2}, \quad (13)$$

$$\delta H'(z) = H_0 \left[\frac{\delta D''(z)}{D'(z)^2} - \frac{2D''(z)\delta D'(z)}{D'(z)^3} \right], \quad (14)$$

$$\delta H''(z) = H_0 \left[\frac{\delta D'''(z)}{D'(z)^2} - \frac{2D'''(z)\delta D'(z)}{D'(z)^3} - \frac{4D''(z)\delta D''(z)}{D'(z)^3} + \frac{6D''(z)^2\delta D'(z)}{D'(z)^4} \right]. \quad (15)$$

Notice that in above formula, we use the same H_0 which has been used to obtain the normalized distance in Eq.(9) and for those quantities with more than one term in uncertainty, we use square root of all terms. For example, for $\delta X = \delta a + \delta b + \delta c + \dots$, the total uncertainty is $\delta X = \sqrt{(\delta a)^2 + (\delta b)^2 + (\delta c)^2 + \dots}$.

Following the same notations we compute the deceleration and jerk parameters as well as the corresponding uncertainties. As a function of $D(z)$, these parameters are:

$$q(z) = -(1+z) \frac{D''(z)}{D'(z)} - 1, \quad (16)$$

$$j(z) = (1+z)^2 \left[-\frac{D'''(z)}{D'(z)} + 3\left(\frac{D''(z)}{D'(z)}\right)^2 \right] - 2(1+z) \frac{D''(z)}{D'(z)} + 1 \quad (17)$$

and as a function of $H(z)$,

$$q(z) = (1+z) \frac{H'(z)}{H(z)} - 1, \quad (18)$$

$$j(z) = (1+z)^2 \left[\frac{H''(z)}{H(z)} + \left(\frac{H'(z)}{H(z)}\right)^2 \right] - 2(1+z) \frac{H'(z)}{H(z)} + 1. \quad (19)$$

In the case of Λ CDM model, namely $H(z) = H_0 E(z) = H_0 [\Omega_{m0}(1+z)^3 + \Omega_{\Lambda0}]^{1/2}$ the cosmokinetic parameters become $q_\Lambda(z) = \frac{3}{2}\Omega_m(z) - 1$ and $j_\Lambda(z) = 1$, where $\Omega(z) = \Omega_0(1+z)^3/E(z)^2$ and $\Omega_{m0} + \Omega_{\Lambda0} = 1$ ².

Lastly, we remind the reader the basic steps of our method (see section II). First the normalized distances $D(z)$ data are given as input to the GAPP code [41]. Second we reconstruct the functional form of $D(z)$ and finally we compute the rest of the cosmological quantities. During the process we consider that the aforementioned data-sets can be treated as statistically

¹ For the rest of the paper $D(x)$ plays the role of $f(x)$.

² For the Λ CDM model we utilize $\Omega_{m0} = 0.3$.

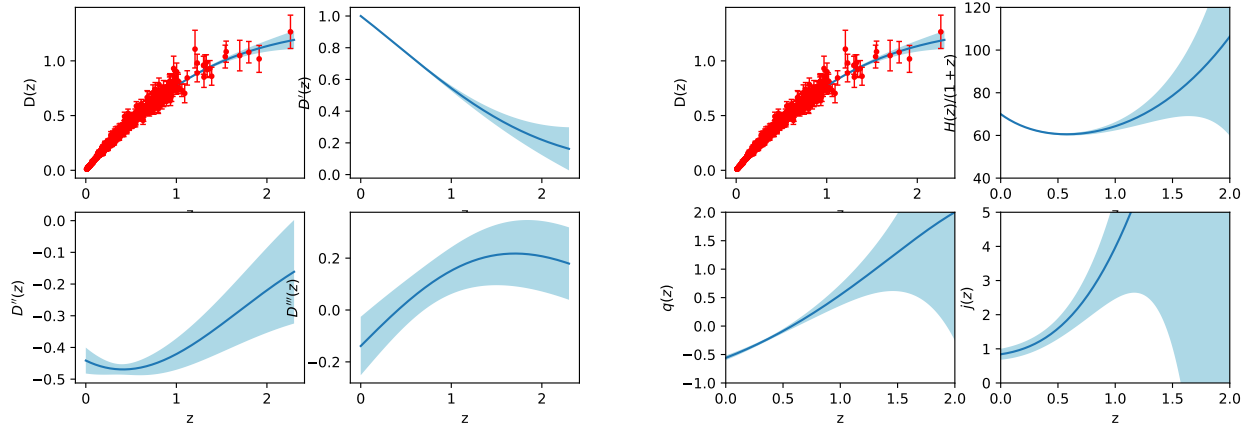


FIG. 1: Left panel: Reconstruction of $D(z)$, data points and its first, second and third derivatives. Right panel: Reconstruction of $D(z)$, the Hubble function, deceleration and jerk parameters as a function of redshift for SNIa data only with the Gaussian kernel.

independent measurements. This assumption is a rather strong statement given that for example the SNIa, QSO and GRB data are sensitive to luminosity distances and there might be spatial overlap between the various probes, hence this could lead to correlations that might affect the statistical analysis. While this is an important point, unfortunately at the moment there is no standard way to account for it given the lack of the full correlation matrix among the different samples. Therefore, following standard lines we have assumed that the different data-sets are uncorrelated. Within this framework, the corresponding parameter space is given by (H_0, q_0, j_0) .

IV. RESULTS AND DISCUSSION

In this section, we discuss the main results of our analysis. Specifically, in Table (I) we provide an overall presentation of the cosmographic parameters at the present epoch. In the left panel of Fig.(1) we present the evolution of the reconstructed $D(z)$ and its derivatives when using the Gaussian kernel and SNIa data. As expected $D'(z)$ decreases as a function of z , hence due to Eq.(10) the Hubble parameter is an increasing function. In the right panel of Fig.(1) we plot the cosmokinetic parameters $H(z)/(1+z)$, $q(z)$ and $j(z)$ as a function of redshift. Moreover in the case of Matern kernels $\nu = 7/2$ and $\nu = 9/2$ the aforementioned parameters are shown in Figs.(2) and (2) respectively. We observe that the evolution of the kinetic parameters are almost the same with those of Gaussian kernel.

However, when combined SNIa with other probes, such as GRBs, the situation becomes different. Indeed, for SNIa/GRBs we plot in Fig.(3) $D(z)$ and its derivatives versus redshift using the Gaussian (left panel) and Matern $\nu = 7/2$ (right panel) kernels. For both cases we observe that in the evolution of the corresponding derivatives appears oscillations. It is easy to check that the first derivative of $D(z)$ crosses the zero line several times, hence the cosmokinetic parameters diverge at these points. Notice that utilizing the Matern $\nu = 9/2$ kernel the results remain unaltered. We argue that although GRBs may help to reconstruct the cosmic expansion up to $z \sim 10$, however there are practical difficulties in achieving this goal in the case of Gaussian process.

Moreover, the results of SNIa/QSO combination are presented in Fig.(4) and Tab.(I). In this case, we observe that $D(z)$ slowly decreases prior to $z \sim 3$, hence a small oscillation appears at that redshift. Furthermore, we find that both Gaussian and Matern kernels provide similar results and in contrast to SNIa/GRB case, here the first derivative of the $D(z)$ does not cross the zero line at 1σ level.

Lastly, we combine SNIa, GRBs and QSOs in order to compute the reconstructed comoving distance for all kernels. As an example in Fig.(5) we plot the evolution of $D(z)$ and the corresponding derivatives in the case of Matern $\nu = 7/2$ kernel. Again we verify that there are epochs which are located at large redshifts and for which $D'(z)$ crosses the zero line (similar behavior is found for the other kernels).

Now we focus on Tab. (I) which shows the cosmokinetic parameters at the present time for various data and kernels explored in this study. Considering only the traditional standard candles (SNIa), we find that the Hubble constant is close to 70Km/sec/Mpc regardless the form of kernel, while q_0 and j_0 are consistent (within 1σ) with those of ΛCDM . Combining SNIa and GRB data, we find that the value of H_0 does not change significantly and it remains close to 70Km/sec/Mpc . In the case of Gaussian kernel, the current value of the deceleration parameter is in agreement with that of ΛCDM at 1σ level. For the Matern's kernels the extracted value of q_0 is marginally consistent with ΛCDM with $q_0 < q_{\Lambda,0}$. Concerning j_0 , our results are similar to those of

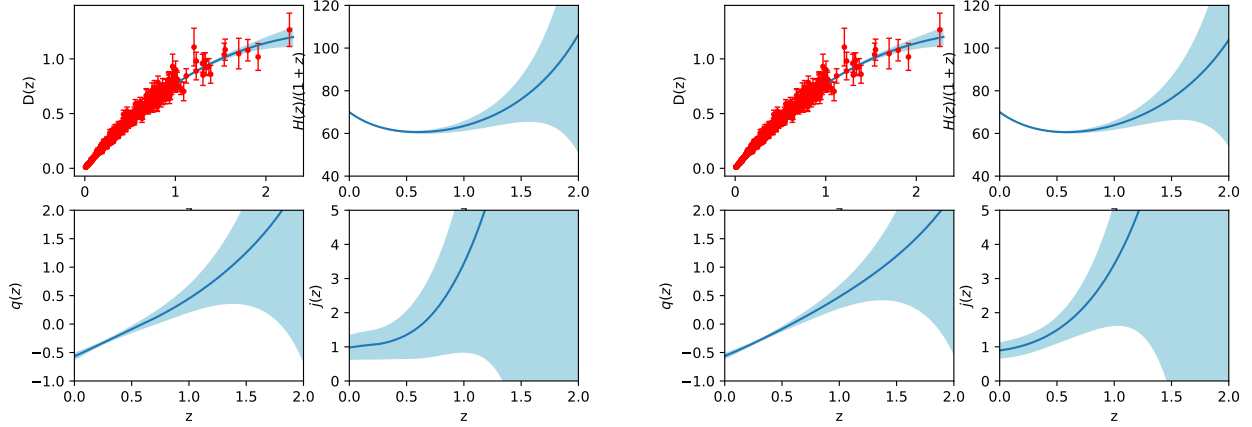


FIG. 2: Left panel: The cosmokinetic parameters as a function of redshift using Matern ($\nu = 7/2$) kernel for SNIa only data. Right panel: The cosmokinetic parameters as a function of redshift using Matern ($\nu = 9/2$) kernel for SN only data.

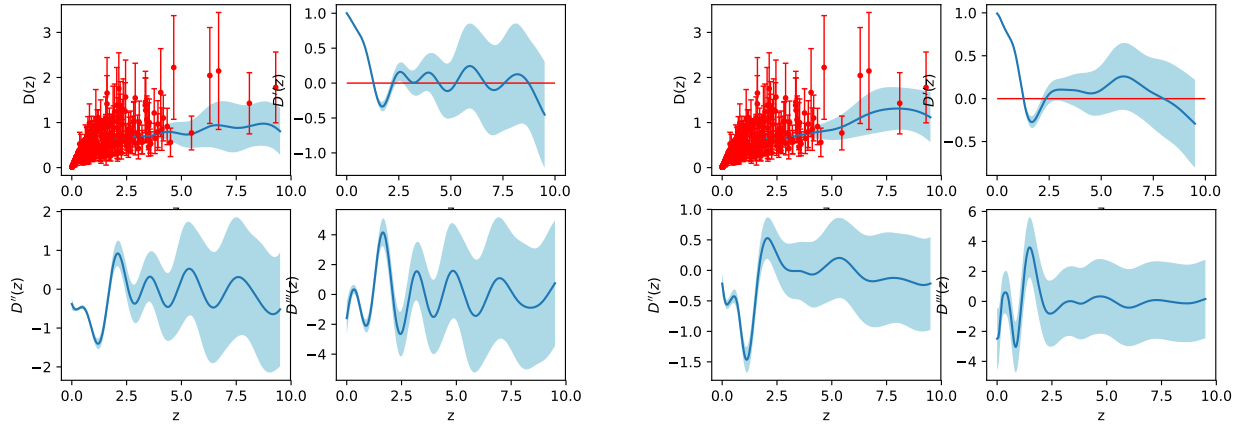


FIG. 3: Left panel: The reconstruction of $D(z)$ and its derivatives as a function of redshift using Gaussian kernel by considering SNIa and GRBs. Right panel: The same plot using Matern ($\nu = 7/2$) kernel and the same data set.

[1], however the corresponding uncertainties are larger (by a factor of 2.5-4) than those of [1], implying that the extracted jerk parameters are consistent with the predictions of Λ CDM at 2σ level. Combining SNIa and QSO datasets, we find that for all kernels the cosmokinetic parameters (q_0, j_0) are in a good agreement (with 1σ) with those of Λ CDM model.

Finally, in the case of the Gaussian kernel the combination SNIa/QSOs/GRBs indicates that the extracted values of q_0 and j_0 are $\sim 3\sigma$ away from those of Λ CDM. However, the opposite situation holds in the case of Matern's kernels, namely both q_0 and j_0 are consistent (due to large uncertainties) with the predictions of Λ CDM. In a nutshell, for the usual standard candles (SNIa data) and for the combination SNIa/QSOs we find that the cosmokinetic parameters (q_0, j_0) extracted from the Gaussian process are consistent with Λ CDM. However, including GRBs in the analysis we find a tension of the Λ CDM model which lies between 2 and 3 σ levels respectively. Moreover, the combined SNIa/QSO/GRB analysis shows that the choice of the kernel function might affect the amount of tension. Indeed in the case of Matern's kernels we produce cosmokinetic parameters which are consistent with those of Λ CDM, while using the Gaussian kernel it seems that the Λ CDM model is in tension with the measurements (q_0, j_0).

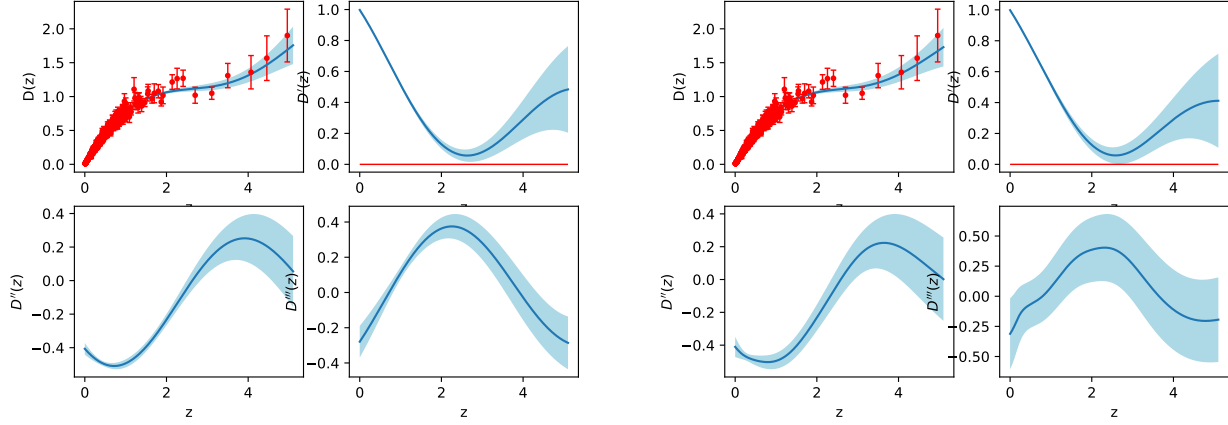


FIG. 4: Left panel: The reconstruction of $D(z)$ and its derivatives as a function of redshift using Gaussian kernel by considering SNIa and QSOs. Right panel: The same plot using Matern ($\nu = 7/2$) kernel and the same data set.

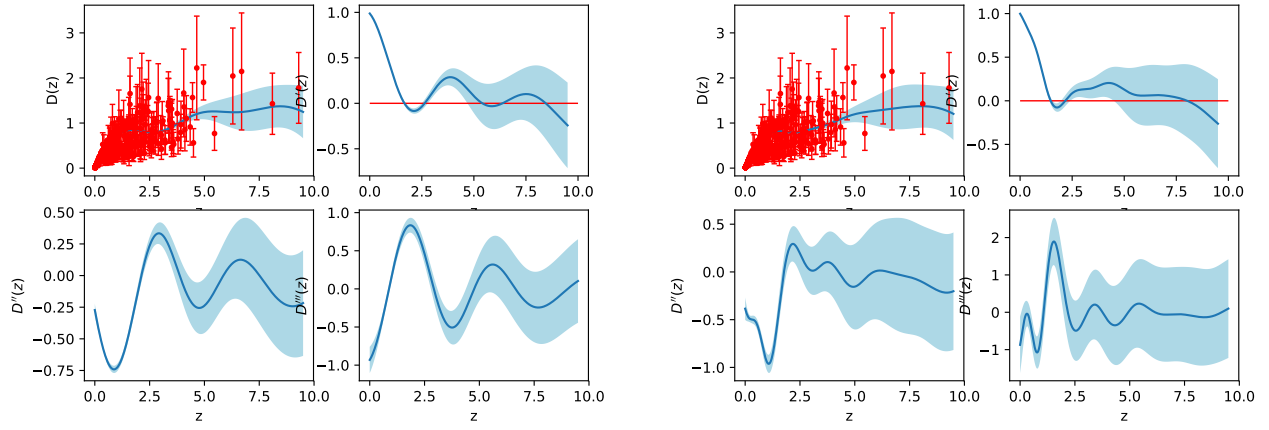


FIG. 5: Left panel: The reconstruction of $D(z)$ and its derivatives as a function of redshift using Gaussian kernel for all data set. Right panel: The same plot using Matern ($\nu = 7/2$) kernel and the same data set.

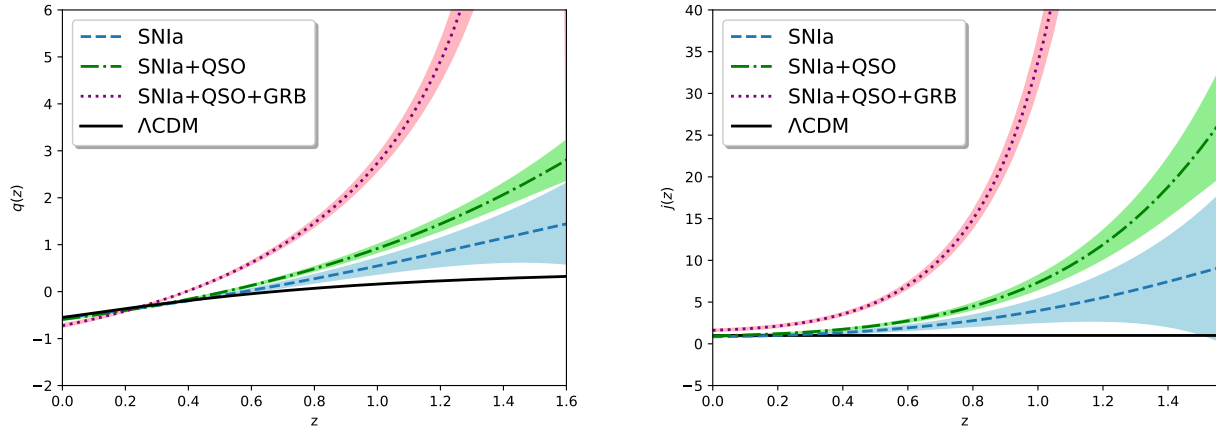


FIG. 6: Left panel: Reconstruction of $q(z)$ using different data sets and considering the Gaussian kernel. Right panel: Reconstruction of $j(z)$. In the case of Λ CDM model we use $\Omega_{m0} = 0.3$ (see solid black lines).

Kernel Data set	Gaussian	Matern $\nu = 7/2$	Matern $\nu = 9/2$
SNIa	$H_0 = 70.00 \pm 0.38$	$H_0 = 69.98 \pm 0.46$	$H_0 = 69.98 \pm 0.42$
	$q_0 = -0.558 \pm 0.04$	$q_0 = -0.567 \pm 0.06$	$q_0 = -0.561 \pm 0.05$
	$j_0 = 0.84 \pm 0.16$	$j_0 = 0.98 \pm 0.36$	$j_0 = 0.89 \pm 0.23$
SNIa+GRBs	$H_0 = 69.92 \pm 0.72$	$H_0 = 70.49 \pm 0.85$	$H_0 = 70.28 \pm 0.77$
	$q_0 = -0.62 \pm 0.15$	$q_0 = -0.79 \pm 0.20$	$q_0 = -0.73 \pm 0.17$
	$j_0 = 2.26 \pm 1.1$	$j_0 = 3.21 \pm 2.1$	$j_0 = 2.80 \pm 1.4$
SNIa+QSOs	$H_0 = 70.17 \pm 0.35$	$H_0 = 70.13 \pm 0.45$	$H_0 = 70.15 \pm 0.40$
	$q_0 = -0.59 \pm 0.03$	$q_0 = -0.58 \pm 0.06$	$q_0 = -0.59 \pm 0.05$
	$j_0 = 0.96 \pm 0.13$	$j_0 = 0.99 \pm 0.33$	$j_0 = 0.95 \pm 0.21$
SNIa+GRBs+QSOs	$H_0 = 70.86 \pm 0.42$	$H_0 = 70.22 \pm 0.69$	$H_0 = 70.12 \pm 0.63$
	$q_0 = -0.72 \pm 0.05$	$q_0 = -0.66 \pm 0.14$	$q_0 = -0.62 \pm 0.11$
	$j_0 = 1.62 \pm 0.2$	$j_0 = 1.98 \pm 1.2$	$j_0 = 1.55 \pm 0.81$

TABLE I: Cosmokinetic parameters at present time for different data sets and kernels.

A. Cosmokinetic parameters at high redshits

Apart from (q_0, j_0) it is useful to study the cosmokinetics parameters at high redshifts. For the Gaussian kernel we plot in Fig.(6) the evolution of $q(z)$ and $j(z)$ in the case of SNIa (blue dashed line), SNIa/QSO (green dot-dashed) and SNIa/QSO/GRBs (magenta dotted curve). For comparison we also plot $q_\Lambda(z)$ and $j_\Lambda(z)$ (see solid lines). Since $D'(z)$ may cross the zero line prior to $z \sim 2$ we prefer to focus on $1 < z < 2$. Obviously, a strong deviation from the Λ CDM predictions is observed in the case of SNIa/QSO and SNIa/QSO/GRBs. We also checked that this result persists regardless the form of the kernel. Although the situation regarding the cosmokinetic tension is not so clear in the present epoch, at high redshifts there is a clear indication that such a tension really exists. Especially, the jerk parameter clearly points to this direction, hence the possibility of having new Physics is not excluded by the present analysis. Notice that, our results are in agreement with those of [1, 2] who found that the deviation from the flat Λ CDM becomes strong at high redshifts ($z > 1$). Combining our model-independent parametrization of the Hubble Diagram with those of [1, 2] we conclude that the deviation from the concordance Λ CDM model is due to new Physics.

V. CONCLUSION

It is well known that the concordance Λ CDM model fits accurately the current cosmological data [7], nonetheless it has been proposed that the model is not without its problems. Indeed there are indications that the Λ CDM model is in tension with some important measurements [32, 33], namely the Hubble constant H_0 and the present value of the mass variance at $8h^{-1}\text{Mpc}$, namely σ_8 . In this context, Lusso *et al.* [1] using a combined Hubble diagram of SNIa, Quasars, and Gamma-Ray Bursts (GRBs) found a $\sim 4\sigma$ tension between the best fit cosmokinetic parameters with respect to those of Λ CDM (see also [2]). Whether the above tensions are the result of yet unknown systematic errors or indicate some underlying new Physics is still an open issue. Therefore, on this subject an intense debate is taking place in the literature and the aim of the present work is to contribute to this debate.

In particular, we combined the traditional standard candles (SNIa data) with other extragalactic sources (Quasars and GRBs) to reconstruct, in a model independent way, the Hubble diagram to as high redshifts as possible and to compute the corresponding cosmokinetic parameters at the present epoch, namely deceleration q_0 and jerk j_0 parameters. Using only the SNIa data we found that the cosmokinetic parameters (q_0, j_0) extracted from the Gaussian process are consistent with those of Λ CDM. Also in the case of SNIa/QSO combination, we found that for all kernels the cosmokinetic parameters are in a very good agreement (with 1σ) with those of Λ CDM model.

On the other hand combining SNIa with Quasars and GRBs we revealed some tension, which lies between 2σ and 3σ levels, depending on the kernel choice. Finally, focusing our analysis on high redshifts ($z > 1$) we found that the corresponding cosmokinetic parameters significantly deviate from those of Λ CDM. Overall the combination of the present work with those of [1, 2] provide a complete investigation of the so called Λ CDM "tension". The three works, which are model independent, clearly suggest that the discrepancy between the Hubble diagram data (especially for $z > 1$) and the predictions of the concordance

Λ CDM model is the result of some underlying new Physics.

-
- [1] E. Lusso, E. Piedipalumbo, G. Risaliti, M. Paolillo, S. Bisogni, E. Nardini, and L. Amati, *Astron. Astrophys.* **628**, L4 (2019), [arXiv:1907.07692 \[astro-ph.CO\]](#) .
- [2] G. Risaliti and E. Lusso, *Nat. Astron.* **3**, 272 (2019), [arXiv:1811.02590 \[astro-ph.CO\]](#) .
- [3] A. G. Riess, A. V. Filippenko, P. Challis, and et al., *Astron. J.* **116**, 1009 (1998).
- [4] S. Perlmutter, G. Aldering, G. Goldhaber, and et al., *Astrophys. J.* **517**, 565 (1999).
- [5] E. Komatsu, K. M. Smith, J. Dunkley, and et al., *Astrophys. J. Supp.* **192**, 18 (2011).
- [6] Planck Collaboration XIV (Planck Collaboration), *Astron. Astrophys.* **594**, A14 (2016).
- [7] N. Aghanim *et al.* (Planck), (2018), [arXiv:1807.06209 \[astro-ph.CO\]](#) .
- [8] D. J. Eisenstein *et al.* (SDSS Collaboration), *ApJ* **633**, 560 (2005).
- [9] W. J. Percival, B. A. Reid, D. J. Eisenstein, and et al., *Mon. Not. R. Astron. Soc.* **401**, 2148 (2010).
- [10] C. Blake *et al.*, *Mon. Not. Roy. Astron. Soc.* **415**, 2876 (2011), [arXiv:1104.2948 \[astro-ph.CO\]](#) .
- [11] B. A. Reid, L. Samushia, M. White, W. J. Percival, M. Manera, *et al.*, *MNRAS* **426**, 2719 (2012).
- [12] T. M. C. Abbott *et al.* (DES), *Mon. Not. Roy. Astron. Soc.* **483**, 4866 (2019), [arXiv:1712.06209 \[astro-ph.CO\]](#) .
- [13] S. Alam *et al.* (BOSS), *Mon. Not. Roy. Astron. Soc.* **470**, 2617 (2017), [arXiv:1607.03155 \[astro-ph.CO\]](#) .
- [14] H. Gil-Marn *et al.*, *Mon. Not. Roy. Astron. Soc.* **477**, 1604 (2018), [arXiv:1801.02689 \[astro-ph.CO\]](#) .
- [15] O. Farooq, F. R. Madiyar, S. Crandall, and B. Ratra, *Astrophys. J.* **835**, 26 (2017), [arXiv:1607.03537 \[astro-ph.CO\]](#) .
- [16] S. Weinberg, *Reviews of Modern Physics* **61**, 1 (1989).
- [17] P. Peebles and B. Ratra, *Rev. Mod. Phys.* **75**, 559 (2003).
- [18] E. J. Copeland, M. Sami, and S. Tsujikawa, *IJMP* **D15**, 1753 (2006).
- [19] T. Chiba, S. Dutta, and R. J. Scherrer, *Phys. Rev. D* **80**, 043517 (2009).
- [20] L. Amendola and S. Tsujikawa, *Dark Energy: Theory and Observations* (Cambridge University Press, Cambridge UK, 2010).
- [21] A. Mehrabi, *Phys. Rev. D* **97**, 083522 (2018), [arXiv:1804.09886 \[astro-ph.CO\]](#) .
- [22] A. Mehrabi and S. Basilakos, *Eur. Phys. J. C* **78**, 889 (2018), [arXiv:1804.10794 \[astro-ph.CO\]](#) .
- [23] H.-J. Schmidt, *Astron. Nachr.* **311**, 165 (1990).
- [24] G. Magnano and L. M. Sokolowski, *Phys. Rev. D* **50**, 5039 (1994).
- [25] A. Dobado and A. L. Maroto, *Phys. Rev. D* **52**, 1895 (1995).
- [26] S. Capozziello, S. Carloni, and A. Troisi, *Recent Res. Dev. Astron. Astrophys.* **1**, 625 (2003).
- [27] S. M. Carroll, V. Duvvuri, M. Trodden, and M. S. Turner, *Phys. Rev. D* **70**, 043528 (2004).
- [28] S. Weinberg, *Reviews of Modern Physics* **61**, 1 (1989).
- [29] T. Padmanabhan, *Physics Reports* **380**, 235 (2003), [arXiv:hep-th/0212290 \[hep-th\]](#) .
- [30] L. Perivolaropoulos, “Six puzzles for Λ CDM cosmology,” (2008), [arXiv:0811.4684 \[astro-ph\]](#) .
- [31] A. Padilla, “Lectures on the cosmological constant problem,” (2015), [arXiv:1502.05296 \[hep-th\]](#) .
- [32] L. Verde, T. Treu, and A. G. Riess, *Nature Astronomy* **3**, 891895 (2019).
- [33] J. Solà, A. Gómez-Valent, and J. de Cruz Pérez, *Physics Letters B* **774**, 317 (2017), [arXiv:1705.06723 \[astro-ph.CO\]](#) .
- [34] M. Rezaei, M. Malekjani, and J. Solà Peracaula, *Phys. Rev. D* **100**, 023539 (2019), [arXiv:1905.00100 \[gr-qc\]](#) .
- [35] J. Solà Peracaula, A. Gómez-Valent, J. de Cruz Pérez, and C. Moreno-Pulido, *Astrophys. J. Lett.* **886**, L6 (2019), [arXiv:1909.02554 \[astro-ph.CO\]](#) .
- [36] H. Velten and S. Gomes, *Phys. Rev. D* **101**, 043502 (2020).
- [37] K. Liao, A. Shafieloo, R. E. Keeley, and E. V. Linder, (2019), [arXiv:1908.04967 \[astro-ph.CO\]](#) .
- [38] M.-J. Zhang and H. Li, *Eur. Phys. J. C* **78**, 460 (2018), [arXiv:1806.02981 \[astro-ph.CO\]](#) .
- [39] A. Gómez-Valent and L. Amendola, *JCAP* **2018**, 051 (2018), [arXiv:1802.01505 \[astro-ph.CO\]](#) .
- [40] F. Melia and M. K. Yennapureddy, *JCAP* **1802**, 034 (2018), [arXiv:1802.02255 \[astro-ph.CO\]](#) .
- [41] M. Seikel, C. Clarkson, and M. Smith, *JCAP* **1206**, 036 (2012), [arXiv:1204.2832 \[astro-ph.CO\]](#) .
- [42] D. M. Scolnic *et al.*, *Astrophys. J.* **859**, 101 (2018), [arXiv:1710.00845 \[astro-ph.CO\]](#) .
- [43] G. Risaliti and E. Lusso, *Astrophys. J.* **815**, 33 (2015), [arXiv:1505.07118 \[astro-ph.CO\]](#) .
- [44] M. Demianski, E. Piedipalumbo, D. Sawant, and L. Amati, *Astron. Astrophys.* **598**, A113 (2017), [arXiv:1609.09631 \[astro-ph.CO\]](#) .
- [45] M. Demianski, E. Piedipalumbo, D. Sawant, and L. Amati, *Astron. Astrophys.* **598**, A112 (2017), [arXiv:1610.00854 \[astro-ph.CO\]](#) .
- [46] L. Amati and M. Della Valle, *Proceedings, 13th Marcel Grossmann Meeting on Recent Developments in Theoretical and Experimental General Relativity, Astrophysics, and Relativistic Field Theories (MG13): Stockholm, Sweden, July 1-7, 2012*, *Int. J. Mod. Phys. D* **22**, 1330028 (2013), [arXiv:1310.3141 \[astro-ph.CO\]](#) .
- [47] M. Plionis, R. Terlevich, S. Basilakos, F. Bresolin, E. Terlevich, J. Melnick, and R. Chavez, *Mon. Not. Roy. Astron. Soc.* **416**, 2981 (2011), [arXiv:1106.4558 \[astro-ph.CO\]](#) .